Published in final edited form as:
Nat Neurosci. 2005 September ; 8(9): 1169–1178.

Essential role of Bag-1 in differentiation and survival of hematopoietic and neuronal cells

Rudolf Götz[1,§], **Stefan Wiese**[1,§], **Shinichi Takayama**[3], **Guadalupe C. Camarero**[2], **Wilfried Rossoll**[1], **Ulrich Schweizer**[1], **Jakob Troppmair**[2,4], **Sibylle Jablonka**[1], **Bettina Holtmann**[1], **John C. Reed**[3], **Ulf R. Rapp**[2], and **Michael Sendtner**[1,‡]

1 *Institut für Klinische Neurobiologie, University of Wuerzburg, Josef Schneider Str. 11, D-97080 Wuerzburg, Germany;*

2 *Institut für Medizinische Strahlenkunde und Zellforschung (MSZ), University of Wuerzburg, Versbacher Str. 5, D-97078 Wuerzburg, Germany;*

3 *The Burnham Institute, La Jolla, California 92037, USA;*

Abstract

By targeted gene disruption in mice, we show that Bag-1, a co-chaperone for Hsp70 which interacts with C-Raf, B-Raf, Akt, Bcl-2, steroid hormone receptors and other proteins, plays an essential role in survival of differentiating neurons and hematopoietic cells. *Bag-1*$^{-/-}$ mice exhibit massive apoptosis in the fetal liver and developing nervous system. Lack of Bag-1 does not disturb the primary function of Akt or Raf as the phosphorylation of the forkhead transcription factor FKHR and activation of Erk-1/2 are not affected. However, the defect correlates with the disturbance of a tripartite complex formed by Akt, B-Raf and Bag-1, with absence of Bad phosphorylation at Ser136. Furthermore, we observe reduced expression of members of the IAP family. Our data reveal that Bag-1 is an important physiological mediator of extracellular survival signals linked to the cellular mechanisms that prevent apoptosis in hematopoietic and neuronal progenitor cells.

Keywords

stem cell; apoptosis; nervous system; embryonic development

Introduction

Bag-family proteins contain an evolutionarily conserved domain (the “BAG” domain) that allows them to bind and modulate the activity of Heat Shock Protein 70 kDa (Hsp70)-family molecular chaperones[1–4]. Humans and mice contain six genes encoding Bag-family proteins, termed Bag-1 (Rap46), Bag-2, Bag-3 (Bis), Bag-4 (Sodd), Bag-5, and Bag-6 (Scythe)[5].

Several Bag-family proteins have been implicated in control of apoptosis. For example, Bag-1 interacts with the anti-apoptotic protein Bcl-2 and protects a variety of cell types from apoptosis in vitro[6,7]. Over-expression of Bag-1 in neurons reduces stroke injury[8] and, in the retina of mice, it provides enhanced protection from apoptosis in vivo, but only if co-expressed with Bcl-2[9]. Bag-3 (Bis) was also reported to interact with Bcl-2 and reduce apoptosis when co-

‡ Corresponding author: Dr. Michael Sendtner, University of Wuerzburg, Institute for Clinical Neurobiology, Josef-Schneider-Str. 11, D-97080 Wuerzburg, Germany, Tel.: 0049-(0)931-201-49771, Fax: 0049-(0)931-201-49788, Email:sendtner@mail.uni-wuerzburg.de.
§Equal contribution
4Current address: Daniel-Swarowski Research Lab, Dept. Of General and Transplant Surgery, Innsbruck Medical University, Innsbruck, Austria

expressed with this protein[10]. In contrast, Bag-4 (Sodd) reportedly associates with certain Tumor Necrosis Factor (TNF)-family receptors and blocks their signaling[11,12]. Also, Bag-6 (Scythe) can regulate a nuclear pathway that communicates with mitochondria, regulating cytochrome *c* release from these organelles, and thereby controlling apoptosis[13,14].

The mechanisms explaining how Bag-1 inhibits apoptosis are poorly understood, and the physiological role of this protein during development is undefined. In addition to associating with Bcl-2, the Bag-1 protein may act as a scaffold protein that binds C-Raf and possibly also B-Raf at the surface of mitochondria[15,16]. In this context, C-Raf could act as an effector kinase which phosphorylates Bad, in addition to other kinases, in particular Akt which have been shown to act as specific kinases for Bad[17,18]. As a consequence, Bad dissociates from Bcl-X_L and this mechanism appears essential for survival of neurons and other types of cells that depend on exogenous survival factors. However, mice in which Ser112, Ser136 and Ser155 of Bad have been mutated are viable but show enhanced cell death after exposure to proapoptotic stimuli and also a reduced threshold for cytochrome *c* release, thus underlining the importance of this protein for cellular survival[19]. Nevertheless, the extent of developmental cell death is much less in comparison to mice in which the B-Raf kinase has been inactivated[20].

In addition to their role in apoptosis, Bag-family proteins have been shown to be involved in other cellular functions. A longer isoform of Bag-1 containing nuclear targeting sequences associates with several steroid hormone receptors, regulating their transcriptional activity[21]. Both the shorter cytosolic Bag-1 and the longer nuclear Bag1L proteins interact with Hsp70, functioning as co-chaperones[1,22,23]. In this regard, Hsp70 plays a protective role in vivo[24]. Nevertheless, the relative importance of Bag-1 as a cochaperone for Hsp70 in regulating apoptosis in vivo is unknown.

Here, we examined for the first time the in vivo function of a Bag-family gene using targeted gene ablation in mice. Inactivation of the *bag-1* gene has important consequences for survival of hematopoietic and neural stem cells. This massive cell death occurs in association with loss of Bad phosphorylation at Ser136. Surprisingly, phosphorylation of Bad at Ser112 and Ser155 is not altered. Akt kinase activation is not changed, and phosphorylation of the forkhead related transcription factor (FKHR), a specific substrate of Akt kinase appears normal. Thus Bag-1 is not necessary for activation of Akt. Nevertheless, we found that Bag-1 is present as a complex with both B-Raf and Akt in vivo. Formation of this complex is impaired in the *bag-1*$^{-/-}$ mice. Our findings reveal that Bag-1 is essential for survival of stem cells in the developing brain and hematopoietic system and thus represents an important physiological mediator of extracellular survival signals that prevent apoptosis.

Results

Targeted inactivation of the mouse bag-1 locus

A targeting vector was designed and constructed to delete the first two coding exons of *bag-1* (Fig. 1a). This strategy was chosen to disrupt the expression of all known isoforms of Bag-1 (p29, Bag-1S, and Bag-1L)[25] which are generated by alternative usage of start codons (Fig. 1a). G418-resistant ES cell clones were isolated and screened by PCR for homologous recombination. Out of 480 clones, 3 showed the expected band (data not shown) and were subjected to diagnostic Southern blot analysis with a probe corresponding to the 5′ flanking region the recombination construct (Fig. 1b). All three ES cell clones exhibited a 2 kb band corresponding to a mutant *bag-1* allele (Fig. 1b). After injection of these recombinant ES cell lines into C57Bl/6 blastocysts, germline transmitting chimaeras were bred with C57Bl/6 females to generate F1 hybrid (129/SJ × C57Bl/6) heterozygotes. *Bag-1*$^{+/-}$ were viable and fertile. The *bag-1* mutation was transferred to a C57Bl/6 background by further crossbreeding with C57Bl/6 wild-type mice for more than three generations.

Intercrossing of heterozygous animals did not yield live offspring with a *bag-1*$^{-/-}$ genotype (n = 28 matings). *Bag-1*$^{+/-}$ animals were indistinguishable from wild-type littermates. Thus, the mutant allele behaves as a recessive trait that is essential for mouse development. Genotyping of mice from heterozygous intercrosses at embryonic day 12.5 revealed that *bag-1*$^{-/-}$ embryos were still present and viable (Fig. 1c and 2a). In contrast, all *bag-1*$^{-/-}$ embryos appeared highly growth-retarded at embryonic day 13.5, and death of these animals was observed between E12.5 and E13.5 (Fig. 1d). Western blot analysis of E12.5 embryos revealed that disruption of the *bag-1* gene leads to complete loss of all known Bag-1 protein isoforms (p29, p32, p50; Fig. 1e).

Bag-1$^{-/-}$ embryos display defects in the liver and the nervous system

At E12.5, *bag-1*$^{-/-}$ mice showed normal body size in comparison to heterozygous and wild-type littermates (Fig. 2). Histological analysis revealed abnormalities in fetal liver and forebrain. This corresponds to the onset of endogeneous expression, which was found at E11.5 with highest levels in the nervous system and liver[26]. The fetal liver of *bag-1*$^{-/-}$ embryos was smaller in comparison to *bag-1*$^{+/-}$ or *bag-1*$^{+/+}$ littermates, suggesting a defect in hematopoiesis. Moreover, *bag-1*$^{-/-}$ embryos appeared anaemic (Fig. 2a), obviously due to macroscopically detectable defects in erythropoiesis in the fetal liver. In the nervous system, the formation of the telencephalic vesicles, which form a major part of the forebrain, appeared severely disturbed (Fig. 2a). The neuroepithelium forming the telencephalic vesicles was significantly reduced in size (Fig. 2b). The spinal cord and dorsal root ganglia were present. However, the mantel zone of the spinal cord was much thinner than the inner epithelial zone consisting of the ependyme and periependymal cells (Fig. 3a).

In situ TUNEL and propidium iodide staining revealed massive apoptosis in the fetal liver of *bag-1*$^{-/-}$ mice (Fig. 2d) and significantly increased apoptosis in the fetal brain (Fig. 2e,f). Quantification of embryonic liver cells with apoptotic nuclei after propidium iodide (PI) staining revealed that 94.2 ± 6.1 % of nuclei were apoptotic in *bag-1*$^{-/-}$ embryos at E12.5, compared to 0.2 ± 0.2 % in wild-type embryos. Similar results were obtained by TUNEL staining.

We also quantified and compared cell death in the forebrain of *bag-1*$^{+/+}$, *bag-1*$^{-/-}$, *b-raf*$^{+/+}$ and *b-raf-1*$^{-/-}$ embryos. In control *bag-1*$^{+/+}$ and *b-raf*$^{+/+}$ forebrain, 1.8 ± 0.5 % and 1.7 ± 0.5 % of all nuclei were PI-positive and showed condensed nuclei by DAPI staining. In contrast, in *bag-1*$^{-/-}$ forebrain 15.1 ± 1.3 % and in *b-raf*$^{-/-}$ forebrain 6.5 ± 0.8 % of all cells showed PI-positive and condensed nuclei (Fig. 2e,f). First indications of cell death in the neuroepithelium were detected at E10.5 by caspase 3 staining (Supplementary Fig. 1).

Altered survival response of cultured bag-1$^{-/-}$ motoneurons.

In mice, motoneurons become postmitotic between E10 and E13, and during a subsequent period of 5–10 days about half of the newly generated neurons undergo apoptosis[27]. This paradigm of physiological cell death allowed us to investigate the role of Bag-1 in endogenous regulatory pathways for cellular survival. We isolated motoneurons from *bag-1*$^{-/-}$ mice and tested their response to neurotrophic factors. The number of motoneurons that could be isolated from lumbar spinal cord of E12.5 *bag-1*$^{-/-}$ embryos was significantly lower in comparison to wild-type and *bag-1*$^{+/-}$ littermates (Fig. 3b). After plating onto laminin-coated culture dishes, the neurotrophic factors GDNF, BDNF or CNTF (each 1ng/ml) were added. Whereas more than 45 % of the originally plated wild-type motoneurons could be supported by these neurotrophic factors over a period of at least 7 days in culture, survival was severely reduced in *bag-1*$^{-/-}$ motoneurons (Fig. 3c,d,e). Motoneurons from *bag-1*$^{+/-}$ mice showed similar survival responses as wild-type neurons.

Neuronal precursor cells die during differentiation in bag-1$^{-/-}$ mice.

Bag-1 has previously been shown to promote neuronal differentiation in the immortalized CSM14.1 cell line[28]. We therefore investigated whether Bag-1 influences differentiation of motoneurons in developing embryos by analysing spinal cord sections with neuronal markers, including nestin, Islet-1/2 and p75^{NTR}. The number of spinal motoneurons showing Islet-1/2 stained nuclei was strongly reduced in *bag-1*$^{-/-}$ embryos (Fig. 3a). However, motoneurons that expressed p75^{NTR} were still present in *bag-1*$^{-/-}$ mice, although the number of these cells also appeared reduced in spinal cord sections (Fig. 3a). These neurons also stained positive for neurofilament-M (data not shown). Staining of E11.5 and E12.5 spinal cord sections also revealed a reduction of nestin-positive neural precursor cells in *bag-1*$^{-/-}$ mice, in particular in the population of motoneuron-like cells that had already migrated from the ventrolateral part of the spinal cord (Fig. 3a). This phenotype was discrete at E11.5 but became prominent at E12.5.

To investigate the role of Bag-1 for differentiating neurons in more detail, we isolated neural stem cells from forebrain of E11.5 *bag-1*$^{-/-}$ embryos. Initial growth and survival of the neurospheres from E11.5 *bag-1*$^{-/-}$ and *bag-1*$^{+/+}$ mice from the same litters was not different when the cells were cultured with bFGF and EGF on uncoated cell culture dishes to prevent differentiation. After passage 6, the cells were transferred to laminin-coated culture dishes to allow differentiation. The attached cells were fixed at 24 hours after plating and analyzed with nestin antibodies for the presence of neural precursor cells and neurofilament-M antibodies for differentiated neurons. The cells were also labeled with propidium iodide to determine the number of apoptotic cells. Neurospheres from *bag-1*$^{+/-}$ embryos contained 10.4 ± 1.0 % neurofilament-M-positive cells, whereas only 2.6 ± 0.9 % were neurofilament-M-positive in *bag-1*$^{-/-}$ neurospheres (see Fig. 4b,e) ($P < 0.001$). In contrast, nestin-positive cells appeared similar in control and *bag-1*$^{-/-}$ neurospheres (Fig. 4a). The proportion of apoptotic nuclei was determined by PI staining, and was found significantly higher in *bag-1*$^{-/-}$ cells compared to *bag-1*$^{+/-}$ cells (4.5 ± 1.3 % versus 0.5 ± 0.3 %) (Fig. 4f). To more clearly define the differentiation stage when the defect occurs, we determined the number of Pax6-positive and Doublecortin-positive cells (Supplementary Fig. 2a,b). There was a more than 100-fold reduction in the number of Pax6-positive cells in differentiating *bag-1*$^{-/-}$ neural stem cell cultures after 48h. The number of early postmitotic Doublecortin-positive cells in the culture dish was less reduced from 5062 ± 570 in control to 2058 ± 617 in *bag-1*$^{-/-}$ cultures. At that time point, the total number of cells was reduced more than 3-fold in *bag-1*$^{-/-}$ cultures (Supplementary Fig. 2e) while the number of cells with condensed nuclei was significantly enhanced (Supplementary Fig. 2c). Thus, the low percentage of neurofilament-M-positive neurons appears to be caused by cell death of neurons as soon as they differentiate from Pax6-positive neural stem cells (Fig. 4e,f and Supplementary Fig. 2d), rather than by a block to differentiation.

Similar results were obtained with an RNAi approach to reduce the level of Bag-1 in neural stem cells derived from *bag-1*$^{+/+}$ embryos (Fig. 4i,k). This experiment was performed to exclude the possibility that *bag-1* deficiency leads to defects at earlier stages of development before neural stem cells differentiate, so that the observed phenotype is caused by indirect effects or selection of different cell populations. The transfection efficiency for the neural stem cells with an eGFP-C1 reporter plasmid was 54.6 ± 4.6 %. Quantification of the Western blots from neural stem cells transfected with the RNAi oligonucleotide revealed a reduction of Bag-1 protein levels to 45.3 ± 6.8 % when compared to the transfection of the respective scrambled RNAi. Given the transfection efficiency, this indicates a nearby complete loss of Bag-1 within successfully transfected cells (Fig. 4i,k). Immunohistochemical detection of Bag-1 in differentiating neural stem cells transfected with the scrambled RNAi revealed that Bag-1 is present in all cells. When the Bag-1 RNAi was transfected, Bag-1 became undetectable in a

proportion of the cells. These cells showed condensed nuclei indicating that cell death occurs when Bag-1 is down-regulated (Supplementary Fig. 3). When these cells were allowed to differentiate for two days on laminin in the absence of EGF or bFGF, the number of PI-positive cells was significantly elevated in RNAi transfected neural stem cells (5.7 ± 2.7 %) in comparison to scrambled RNAi treated cells (1.0 ± 1.1 %) or vector (pEGFP-C1) alone transfected cells (0.9 ± 0.9 %). While the number of Propidium iodide-positive cells increased, the number of neurofilament-positive cells dropped significantly ($P < 0.01$) in Bag-1 RNAi treated neural stem cells (6.4 ± 2.2 %) in comparison to transfection with the scrambled RNAi sequence (14.2 ± 0.9 %) or transfection of eGFP-C1 (13.2 ± 1.0 %). We conclude that Bag-1 is required for survival of differentiating neural stem cells and that gene ablation and acute interference with gene expression lead to similar phenotypes in cultured stem cells derived from E11.5 mouse forebrain.

Pax6 and Doublecortin are markers of undifferentiated and early differentiating neural progenitors, respectively. Immunhistochemistry of E11.5 spinal cord and brain sections with antibodies for Pax6 and Doublecortin (Dc) revealed that the number of Pax6-positive cells with condensed nuclei is increased in *bag-1*$^{-/-}$ embryos (Fig. 5a,c, Supplementary Fig. 4a,c; Supplementary Table 1). In contrast, the number of Doublecortin-positive cells with condensed nuclei was not increased in *bag-1*−/− embryos. In conclusion; a significant ($P < 0.01$) increase in the number of condensed nuclei was exclusively observed in the fraction of the Pax6-positive cells but not in the more differentiated cell fraction which was Doublecortin-positive (Fig. 5b; Supplementary Fig. 4b,c).

The Raf-Erk-Signalling pathway is not disturbed in bag-1$^{-/-}$ cells.

In order to study the molecular mechanisms of altered neural and hematopoietic stem cell survival in more detail, we first investigated the Raf/MAPK signalling pathway because Bag-1 is known to interact with C-Raf. Phosphorylation of Erk-1/2 in liver from *bag-1*$^{+/+}$ and *bag-1*$^{-/-}$ mice (Fig. 6a,b) as well as in primary embryonic fibroblasts derived from *bag-1*$^{+/+}$ and *bag-1*$^{-/-}$ embryos appeared unchanged. We then tested the activation of the MAPK pathway by stimulating primary fibroblasts from *bag-1*$^{+/+}$ and *bag-1*$^{-/-}$ with insulin-like growth factor-1 (IGF-1). Also, under these conditions, Erk-1/2 activation was normal (Fig. 6b).

Absence of Bag-1 disturbs Bad phosphorylation at Ser136

PI3 kinase is important both for the upregulation of IAPs[29] and for activation of Akt. We therefore investigated phosphorylation of Bad, which has previously been identified as a target of Akt and a potential substrate of a complex between C-Raf and Bag-1[15]. Bad phosphorylation at Ser136 was not detectable by Western blot analysis of *bag-1*$^{-/-}$ liver extracts, using phospho-specific antibodies (Fig. 6c). Similar results were obtained with E11.5 brain extracts (Fig. 6e). In contrast, phosphorylation at Ser112 and Ser155 were not affected by *bag-1* gene ablation (Fig. 6c,e). This suggests that Bag-1 is essential for phosphorylation of Bad at Ser136 in vivo.

We have shown before that B-Raf is essential for survival of developing neurons [29]. In order to investigate the role of B-Raf in this context we compared Bad phosphorylation in protein extracts of E11.5 *bag-1*$^{+/+}$, *bag-1*$^{-/-}$, *b-raf*$^{+/+}$ and *b-raf*$^{-/-}$ brain. Pulldown of Bad revealed absence of Ser136 phosphorylation in *bag-1*$^{-/-}$ and *b-raf*$^{-/-}$ brain while the phosphorylation of Ser112 and Ser155 remained unaffected (Fig. 6e).

Bag-1 deficiency does not disturb Akt activity

Akt and other kinases phosphorylate Bad at Ser112, and Akt specifically phosphorylates at Ser136 in response to activation of the PI3-K pathway[17]. Therefore, we tested whether absence of Bag-1 protein leads directly or indirectly to abnormalities in Akt kinase activation. Analysis

of *bag-1*$^{+/+}$ and *bag-1*$^{-/-}$ fetal liver and brain extracts showed that Akt phosphorylation at Thr308 and Ser473 was normal (Fig. 6d). These sites are known to activate Akt in response to PI3-K, a mechanism which seems important to couple tyrosine kinase signaling to Bad phosphorylation, thereby preventing cellular apoptosis. Thus, the pathway which leads to activation of Akt kinase appears intact in *bag-1*$^{-/-}$ animals. We then investigated whether Akt kinase activity is impaired by testing phosphorylation of the forkhead homologous transcription factor FKHR, a specific target of Akt kinase[30]. FKHR phosphorylation was indistinguishable in E12.5 *bag-1*$^{-/-}$ and *bag-1*$^{+/+}$ brain and liver (Fig. 6d), indicating that *bag-1*-deficiency does not reduce kinase activity of Akt. Thus, lack of Bad phosphorylation at Ser136 is caused by other mechanisms than a general defect in activation and enzymatic activity of Akt.

Altered expression of IAPs in liver and brain of bag-1$^{-/-}$ embryos.

Previous studies have shown that neurotrophic factor-mediated survival of developing neurons depends on B-Raf and induction of IAP family gene expression[20]. Similar observations were made in studies investigating survival of endothelial cells in response to VEGF[29]. We therefore studied expression of IAPs in developing brain and hematopoietic cells of the fetal liver in E12.5 *bag-1*$^{-/-}$ embryos. Expression of IAP-2 (Fig. 6g) and X-IAP (Fig. 6h) was highly reduced in brain and liver of *bag-1*$^{-/-}$ embryos. In contrast, IAP-1 (Fig. 6f) expression was not reduced in the brain but only in the liver.

Absence of Bag-1 leads to altered association of B-Raf, Akt and Bad.

C-Raf specifically interacts with Bag-1, and it has been suggested that C-Raf also phosphorylates Bad at so far undefined serine residues[15,31]. Notably, B-Raf appears more important than C-Raf[20] for survival of developing neurons, and *b-raf*$^{-/-}$ mice resemble *bag-1*$^{-/-}$ mice in that the survival response to neurotrophic factors in embryonic motoneurons is strongly reduced and expression of members of the *IAP* gene family is disturbed[20]. Therefore, we analysed whether B-Raf also interacts with Bag-1. In PC12 pheochromocytoma cells, endogeneous B-Raf and Bag-1 both interact with Hsp70 (Fig. 7a). In addition, B-Raf and Bag-1 could be mutually co-immunoprecipitated (Fig. 7b,c). The same effect was observed for C-Raf but not for A-Raf. Additionally, we investigated whether B-Raf and Akt kinase could be co-immunoprecipitated, based on a prior report suggesting that these two kinases can associate within a protein complex[20,32]. When endogenous B-Raf or Bag-1 were precipitated from PC12 cells, we detected Akt (Fig. 7d), thus confirming data on the interaction of Akt and B-Raf after over-expression in HEK293 cell extracts[33].

To analyze the interactions between Bad, Akt, B-Raf and Hsp70 in wild-type and *bag-1*$^{-/-}$ cells in more detail, we prepared protein lysates from E11.5 *bag-1* heterozygous intercross embryos. In wild-type brain extracts we observed strong interaction between B-Raf and Akt was observed(Fig. 7e). The interaction between B-Raf and Akt was absent in *bag-1*$^{-/-}$ embryos (Fig. 7e), indicating that Bag-1 acts as a scaffold to bring these two kinases into one complex or that the co-chaperone activity of Bag-1 is required for formation of this complex. The interaction between Akt and Bad was also weaker in brain extracts from *bag-1*$^{-/-}$ mice (Fig. 7e,g). We also investigated the interaction between Bad and Hsp70. This interaction was absent in extracts from *bag-1*$^{-/-}$ mice (Fig. 7f), suggesting that Hsp70 together with Bag-1 is involved in a complex which brings Akt in proximity of its target Bad. In confirmation of this hypothesis, we also found that the interaction between B-Raf and Hsp70 was disrupted in *bag-1*$^{-/-}$ embryo extracts (Fig. 7f).

In order to study whether B-Raf also interacts with Bad, we performed additional immunoprecipitation experiments. With antibodies against B-Raf, the Bad protein could only be coprecipitated in wild-type but not in *bag-1*$^{-/-}$ embryo extracts (Fig. 7h). Levels of Bad protein do not differ between controls and *bag-1*$^{-/-}$ embryos.

Absence of Bag-1 leads to altered protein distribution of B-Raf and Akt.

To investigate expression and subcellular distribution of Akt and B-Raf in *bag-1*$^{+/+}$ and *bag-1*$^{-/-}$ cells, we focused on motoneurons, as these cells depend on survival signaling at embryonic day 11.5 and can easily be identified in the developing spinal cord. In wild-type animals, most phospho-Akt (P-Akt) immunoreactivity co-localized with cytochrome *c* oxidase at mitochondria-like structures in the cytoplasm (Fig. 8a,c). In contrast, in *bag-1*$^{-/-}$ motoneurons, P-Akt appeared diffusely distributed in the cytoplasm and was much less enriched at mitochondria (Fig. 8b and 9d). Similar results were obtained for subcellular distribution of B-Raf (Fig. 8e,f). We quantified the pixels for P-Akt and B-Raf immunhohistochemistry which overlapped with cytochrome *c* oxidase immunoreactivity in control and *bag-1*$^{-/-}$ cells. This analysis revealed a reduction in the localization of P-Akt or B-Raf at mitochondria in the *bag-1*$^{-/-}$ motoneurons (Fig. 8g-h). Thus, Bag-1 appears important for concentrating B-Raf and Akt at mitochondria[33], a site where phosphorylation of Bad and probably also the activation of pathways leading to IAP upregulation are expected to occur.

Discussion

Here we report that gene knockout of *bag-1* in mice causes massive cell death in the embryonic liver and severe defects in differentiation and survival of neuronal cells. In the nervous system, enhanced cell death occurs in Pax6-positive neural stem cells. The abnormal cell death of neural stem cells and hematopoietic precursor cells correlates with absence of phosphorylation of the proapoptotic protein Bad at Ser136. This site has previously been recognized as a specific target for Akt kinase after activation by neurotrophic and other pro-survival signals involving tyrosine kinase receptors and PI3-K stimulation. In addition, levels of X-IAP and IAP-2 are reduced, as previously observed in *b-raf*$^{-/-}$ mice[20]. The function of Raf kinases in activation of MEK/ERK is not blocked by the absence of Bag-1, and phosphorylation of the forkhead transcription factor FKHR, a specific target of the Akt kinase, is also unchanged. However, absence of Bag-1 leads to altered subcellular distribution of B-Raf and Akt. This could disturb the specific function of these kinases i.e. in phosphorylating Bad at Ser136, a process which takes place at mitochondria[19].

Bag-1 has originally been identified as a Bcl-2-interacting protein that potentiates its survival promoting activity[15]. Bag-1 also specifically interacts with C-Raf and, as shown here, with B-Raf, but not with A-Raf. Binding of C-Raf to Bag-1 stimulates its kinase activity and thus potentiates signals for cellular growth and differentiation. Therefore it was hypothesized that mitochondrial Raf, activated by a Bag-1-dependent mechanism, acts as effector kinase of Bcl-2 phosphorylating targets such as Bad[15]. However, gene knockout of *bcl-2* does not lead to enhanced neuronal apoptosis of developing motoneurons[34] which are severely affected in *bag-1*$^{-/-}$ embryos, suggesting either that other members of the Bcl-2 family also interact with Bag-1 and thus compensate for *bcl-2* deficiency or that Bag-1 acts independently from Bcl-2 in developing neurons to mediate neurotrophic survival effects. Phosphorylation of Bad leads to dissociation from a complex with Bcl-X_L at the mitochondrial surface, and the protein is sequestered to the cytosol by the phosphoserine binding protein 14-3-3[35]. In another experimental paradigm it has been shown that deficiency of merosin leads to decreased levels of Bag-1 and reduced levels of Bad phosphorylation[36]. Thus, this process appears important for cellular survival, in particular of neurons and hematopoietic cells. The phenotype observed in our study with *bag-1*$^{-/-}$ mice therefore is consistent with a model in which Bag-1 cooperates with Raf kinases in phosphorylation of Bad, thus inhibiting apoptosis.

Is has been speculated that Raf kinases could also phosphorylate Bad and thus act in parallel or together with Akt in this function. However, attempts to identify specific sites in Bad that are phosphorylated by C-Raf in vivo have not been successful. Phosphorylation in vitro of recombinant Bad by C-Raf occurs with low efficiency, in contrast to phosphorylation by

activated Akt kinase[31]. Thus Akt kinase is more robust at phosphorylating Bad at Ser136. Nevertheless, B-Raf also appears essential for neuronal survival as isolated neurons from *b-raf*$^{-/-}$ mice cannot survive in the presence of neurotrophic factors[20]. *B-raf*$^{-/-}$ brain extracts also show a strong reduction in Bad phosphorylation at Ser136 similar to what is observed in the *bag-1*$^{-/-}$ brain and liver extracts. It remains open whether Akt or B-Raf is responsible for Bad Ser136 phosphorylation. The observation that Ser136 phosphorylation is also reduced in *b-raf*$^{-/-}$ brain suggests that B-Raf is necessary either directly or indirectly within a complex with Bag-1 in order to phosphorylate Bad at Ser136 at the surface of mitochondria.

In the absence in *bag-1*$^{-/-}$, a complex between Akt, B-Raf and Hsp70 is disrupted and B-Raf and Akt kinase loose their contact with mitochondria. These findings suggest that Bag-1 plays a role in assembly of B-Raf, Akt and Hsp70 to a complex which is important for Bad phosphorylation and for other mechanisms which regulate induction and execution of cell death. We do not know whether Hsp70 and the function of a chaperone complex involving these molecules is deficient in *bag-1*$^{-/-}$ cells. At least, Hsp70 protein levels are not decreased in brain and liver of E12.5 *bag1*$^{-/-}$ mice (Fig. 4a), when cell death is prominent. However, the observation that Bad is not phosphorylated at Ser136 in *bag-1*$^{-/-}$ tissues, whereas phosphorylation at Ser112 and Ser155 is normal, suggests that Bag-1 functions in a way which goes beyond activation of either Raf or Akt kinases. Also our findings that activation of the MAPK pathway and FKHR phosphorylation is normal suggest that Bag-1 is not necessary for the activity of Raf kinases and Akt. On the other hand, we cannot exclude that the presence of Bag-1 and Hsp70 is necessary for the activity of B-Raf and Akt specifically in the context of Bad phosphorylation at Ser136. Alternatively, it could be that Bag-1 and Hsp70 are necessary for changing the conformation of Bad so that Ser136 is accessible for phosphorylation by Akt or B-Raf kinases. Therefore, we propose a model that Bag-1 and Hsp70 need to be present in a complex on the surface of mitochondria in order to allow phosphorylation of Bad at Ser136 by Akt and/or B-Raf (see model in Supplementary Fig. 5a,b). If such a complex exists it will be interesting to see what the activity of the kinases in this complex actually is.

Though Bag-1 is required for proper targeting of Raf kinases and Akt to the mitochondria and for Bad Ser136 phosphorylation, the absence of Bag-1 probably has also other effects on cell survival as well. In this regard mice in which Bad Ser112, -136 and -155 are mutated to alanines show enhanced cell death under various conditions but the phenotype of these mice is much less severe than the phenotype of *bag-1*$^{-/-}$ or *b-raf*$^{-/-}$ mice[19]. This indicates that Bad phosphorylation at Ser136 is not the only event regulating survival of neuronal and hematopoietic cells. In contrast to *bad* mutant mice, *b-raf*$^{-/-}$ mice show excessive cell death in particular in the nervous system and thus resemble *bag-1*$^{-/-}$ mice. Neurotrophin-induced expression of IAPs has previously been shown to be essential for neuronal survival and this survival pathway is also dependent on B-Raf [37]. We observe that IAP gene expression is disturbed in *bag-1*$^{-/-}$ embryos in a similar manner as in *b-raf*$^{-/-}$ mice[20]. IAP gene expression is regulated by NfkB[38], and the massive cell death phenotype in the liver of *bag-1*$^{-/-}$ embryos resembles that of mouse mutants with disturbed NfkB signalling. *RelA*$^{-/-}$ mice die at E15 to 16 by massive apoptosis in liver cells[39]. However, in contrast to *bag-1*$^{-/-}$ mice, no major defects were observed in the developing brain of *relA* mutants, and the erythropoietic cells in the liver of *relA*$^{-/-}$ mice appeared unaffected in comparison to *bag-1*$^{-/-}$ mice. Whether this is due to the observation that additional signaling pathways are affected in *bag-1*$^{-/-}$ mice such as the pathway leading to Bad phosphorylation at Ser136 remains to be determined.

Notably, the initial development and generation of neuronal precursor cells is much less affected in *bag-1*$^{-/-}$ mice before neuronal cells differentiate and become postmitotic. This observation suggests that Bag-1 becomes important at a critical point of development when neurons and other cells become competent to die [40]. Observations that phosphorylation of ERKs is normal in *bag-1*$^{-/-}$ mice is consistent with the observation that general growth of the

embryos up to embryonic day 12 is not significantly altered. We have previously observed that most of the B-Raf but also C-Raf kinase immunoreactivity in postmitotic motoneurons are localized at mitochondria. Our data that C-Raf and B-Raf can be co-precipitated with antibodies against Bag-1 suggest that Bag-1 becomes highly important for these postmitotic cells after they have become competent to die. The observation that the subcellular distribution of Akt kinase also changes and much less Akt kinase is located at mitochondria of *bag-1*$^{-/-}$ neurons could provide an explanation for the massive apoptosis that occurs at this developmental stage in *bag-1*$^{-/-}$ mice.

In conclusion, the phenotype of *bag-1*−/− mice suggests that this molecule plays a central role for survival of neurons and other cell types once they become competent to die. The interaction of Bag-1 with steroid receptors, Hsp70 and Raf kinases provides a structural counterpart to the observation that cellular signaling pathways involving these molecules play together in regulating cellular survival. Lack of Bag-1 disrupts such coordinated functions, finally leading to massive apoptosis in the nervous system and other organs during development.

Experimental Procedures

Generation of bag-1$^{-/-}$ mice.

The procedure for generating *bag-1*$^{-/-}$ mice is described in detail in the Supplementary Notes. All animal procedures were approved by the Bavarian State authorities for animal experimentation.

Cell culture techniques.

Cultures of spinal motoneurons from embryonic day 12.5 mice were prepared by a panning technique using a monoclonal rat anti-p75^{NTR} antibody (Chemicon) according to a previously published method[20].

PC12 cells were propagated under standard medium conditions (DMEM, 10 % horse serum, 5 % fetal calf serum, FCS). For immunoprecipitation experiments the cells were synchronised at low serum and treated for 24 hours with NGF. The cells were lysed (5×10^6 cells for each immunoprecipitation experiment initially) and the extracts treated with the indicated precipitation antibodies.

Cultures of neurospheres from embryonic day 12.5 and 11.5 mice were prepared by dissecting the forebrain as described in detail in the supplementary notes.

Primary embryonic fibroblasts were isolated from E12.5 *bag-1*$^{+/+}$ and *bag-1*$^{-/-}$ single embryos using standard techniques as described in the Suppplementary notes. The embryos were decapitated and the intestinal organs removed. The embryo bodies were washed three times in PBS and treated with 0.1 % Trypsin/EDTA (Invitrogen) for 10 min at 37°C. Each single embryo body was passed through a 21 gauche needle and cells transferred to individual culture dishes. The plates were filled with DMEM medium containing 10 % FCS and 1 % non essential amino acids (NEAA, Invitrogen). Cells were passaged 3 times, then put on individual 10 cm cell culture plates and grown under low serum conditions (0.5 % FCS) for 24 h prior to stimulation with IGF-1 for the indicated time points.

Protein isolation, Western blotting and immunoprecipitation.

Embryonic tissue was obtained from litters derived from intercrosses of *bag-1*+/− mice. After lysis in RIPA buffer, electrophoresis and blotting, the membranes were stained with Ponceau S (Sigma) to mark molecular mass standard proteins. For immunoprecipitation tissue or cell extracts were precleared with Protein A-Sepharose, and then incubated with 1 μg/ml

appropriate antibody (anti-Akt, anti-B-Raf, anti-Bad; New England Biolabs/Cell Signaling; anti-Bag-1, SantaCruz) overnight. Precipitates were processed according to standard protocols for further Western blot analysis.

Immunofluorescence of cell cultures and tissue sections of embryonic mice.

Vibratome stections and cell cultures derived from 11.5 and 12.5-day-old embryos from *bag-1*$^{+/-}$ intercrosses were processed for immunostaining and confocal microscopic analysis as described in detail in the Supplementary Notes.

RT-PCR for IAP-1, IAP-2 and X-IAP.

RNA from brain and liver of E12.5 mice was isolated by TRIZOL reagent (Invitrogen). For each RT-PCR reaction, 10 ng of RNA was used. RT-PCR was done according to the manufacturer's instructions (Invitrogen) with random hexamer primers. The primer sequences used to amplify IAP-1, IAP-2, X-IAP and elongation factor-1 (EF-1) were used according to earlier published sequences[20].

Calculation and statistics.

Results of neuronal counts were expressed as mean and standard error of the mean (sem) or standard deviation (sd) as indicated. Statistical significance was assessed by t-test or ANOVA followed by Bonferoni's test, using the GraphPad Prism software (San Diego, USA).

Supplementary Material

Refer to Web version on PubMed Central for supplementary material.

Acknowledgements

We are grateful to M. Pfister, J. Marcano and K. Kalus for excellent technical assistance. We thank R. McKay (NIH, Bethesda, ML) for providing the nestin antibody, Thomas Jessell for providing the Islet-1/2 hybridoma (39.4D5) via the DSHB (Iowa) and R. Timpl for kind donation of laminin. This work was supported by the Deutsche Forschungsgemeinschaft, SE 697/3-3, SFB581 TP B4 and B17, The NIH (CA67385), and by the Hermann und Lilly Schilling foundation.

References

1. Takayama S, et al. BAG-1 modulates the chaperone activity of Hsp70/Hsc70. EMBO J 1997;16:4887–4896. [PubMed: 9305631]
2. Bimston D, et al. BAG-1, a negative regulator of hsp70 chaperone activity, uncouples nucleotide hydrolysis from substrate release [In Process Citation]. EMBO J 1998;17:6871–6878. [PubMed: 9843493]
3. Stuart JK, et al. Characterization of interactions between the anti-apoptotic protein BAG- 1 and Hsc70 molecular chaperones. J Biol Chem 1998;273:22506–22514. [PubMed: 9712876]
4. Brehmer D, et al. Tuning of chaperone activity of Hsp70 proteins by modulation of nucleotide exchange. Nat Struct Biol 2001;8:427–432. [PubMed: 11323718]
5. Takayama S, Reed JC. Molecular chaperone targeting and regulation by BAG family proteins. Nat Cell Biol 2001;3:E237–E241. [PubMed: 11584289]
6. Takayama S, et al. Cloning and functional analysis of BAG-1: a novel Bcl-2-binding protein with anti-cell death activity. Cell 1995;80:279–284. [PubMed: 7834747]
7. Wang HG, Reed JC. Bc1-2, Raf-1 and mitochondrial regulation of apoptosis. Biofactors 1998;8:13–16. [PubMed: 9699002]
8. Kermer P, et al. BAG1 over-expression in brain protects against stroke. Brain Pathol 2003;13:495–506. [PubMed: 14655755]
9. Eversole-Cire P, et al. Synergistic effect of Bcl-2 and BAG-1 on the prevention of photoreceptor cell death. Invest Ophthalmol Vis Sci 2000;41:1953–1961. [PubMed: 10845622]

10. Lee MY, et al. Reactive astrocytes express bis, a bcl-2-binding protein, after transient forebrain ischemia. Exp Neurol 2002;175:338–346. [PubMed: 12061864]
11. Jiang Y, Woronicz JD, Liu W, Goeddel DV. Prevention of constitutive TNF receptor 1 signaling by silencer of death domains. SCI 1999;283:543–546.
12. Miki K, Eddy EM. Tumor necrosis factor receptor 1 is an ATPase regulated by silencer of death domain. Mol Cell Biol 2002;22:2536–2543. [PubMed: 11909948]
13. Thress K, Song J, Morimoto RI, Kornbluth S. Reversible inhibition of Hsp70 chaperone function by Scythe and Reaper. EMBO J 2001;20:1033–1041. [PubMed: 11230127]
14. Thress K, Henzel W, Shillinglaw W, Kornbluth S. Scythe: a novel reaper-binding apoptotic regulator. EMBO J 1998;17:6135–6143. [PubMed: 9799223]
15. Wang HG, Takayama S, Rapp UR, Reed JC. Bcl-2 interacting protein, BAG-1, binds to and activates the kinase Raf-1. Proc Natl Acad Sci USA 1996;93:7063–7068. [PubMed: 8692945]
16. Wang HG, Rapp UR, Reed JC. Bcl-2 targets the protein kinase Raf-1 to mitochondria. Cell 1996;87:629–638. [PubMed: 8929532]
17. Datta SR, et al. Akt phosphorylation of BAD couples survival signals to the cell-intrinsic death machinery. Cell 1997;91:231–241. [PubMed: 9346240]
18. Datta SR, et al. 14-3-3 proteins and survival kinases cooperate to inactivate BAD by BH3 domain phosphorylation. Mol Cell 2000;6:41–51. [PubMed: 10949026]
19. Datta SR, et al. Survival factor-mediated BAD phosphorylation raises the mitochondrial threshold for apoptosis. Dev Cell 2002;3:631–643. [PubMed: 12431371]
20. Wiese S, et al. Specific function of B-Raf in mediating survival of embryonic motoneurons and sensory neurons. Nat Neurosci 2001;4:137–142. [PubMed: 11175873]
21. Froesch BA, Takayama S, Reed JC. BAG-1L protein enhances androgen receptor function. J Biol Chem 1998;273:11660–11666. [PubMed: 9565586]
22. Hohfeld J, Jentsch S. GrpE-like regulation of the hsc70 chaperone by the anti-apoptotic protein BAG-1. EMBO J 1997;16:6209–6216. [PubMed: 9321400]
23. Schmidt U, et al. Essential role of the unusual DNA-binding motif of BAG-1 for inhibition of the glucocorticoid receptor. J Biol Chem 2003;278:4926–4931. [PubMed: 12482863]
24. Yenari MA, Giffard RG, Sapolsky RM, Steinberg GK. The neuroprotective potential of heat shock protein 70 (HSP70). Mol Med Today 1999;5:525–531. [PubMed: 10562718]
25. Coldwell MJ, et al. The p36 isoform of BAG-1 is translated by internal ribosome entry following heat shock. Oncogene 2001;20:4095–4100. [PubMed: 11494137]
26. Crocoll A, Blum M, Cato AC. Isoform-specific expression of BAG-1 in mouse development. Mech Dev 2000;91:355–359. [PubMed: 10704864]
27. Lo AC, Houenou LJ, Oppenheim RW. Apoptosis in the nervous system: morphological features, methods, pathology, and prevention. Arch Histol Cytol 1995;58:139–149. [PubMed: 7576866]
28. Kermer P, et al. Bag1 is a regulator and marker of neuronal differentiation. Cell Death Differ 2002;9:405–413. [PubMed: 11965493]
29. Tran J, et al. Marked induction of the IAP family antiapoptotic proteins survivin and XIAP by VEGF in vascular endothelial cells. Biochem Biophys Res Commun 1999;264:781–788. [PubMed: 10544009]
30. Brunet A, et al. Akt promotes cell survival by phosphorylating and inhibiting a Forkhead transcription factor. Cell 1999;96:857–868. [PubMed: 10102273]
31. von Gise A, et al. Apoptosis suppression by Raf-1 and MEK1 requires MEK- and phosphatidylinositol 3-kinase-dependent signals. Mol Cell Biol 2001;21:2324–2336. [PubMed: 11259582]
32. Jablonka S, Wiese S, Sendtner M. Axonal defects in mouse models of motoneuron disease. J Neurobiol 2004;58:272–286. [PubMed: 14704958]
33. Guan KL, et al. Negative regulation of the serine/threonine kinase B-Raf by Akt. J Biol Chem 2000;275:27354–27359. [PubMed: 10869359]
34. Michaelidis TM, et al. Inactivation of the bcl-2 gene results in progressive degeneration of motoneurons, sensory and sypathetic neurons during early postnatal development. Neuron 1996;17:75–89. [PubMed: 8755480]

35. Gross A, McDonnell JM, Korsmeyer SJ. BCL-2 family members and the mitochondria in apoptosis. Genes Dev 1999;13:1899–1911. [PubMed: 10444588]

36. Laprise P, et al. Merosin (laminin-2/4)-driven survival signaling: complex modulations of Bcl-2 homologs. J Cell Biochem 2003;89:1115–1125. [PubMed: 12898510]

37. Wiese S, et al. The anti-apoptotic protein ITA is essential for NGF-mediated survival of embryonic chick neurons. Nat Neurosci 1999;2:978–983. [PubMed: 10526336]

38. Wang CY, Mayo MW, Korneluk RG, Goeddel DV, Baldwin ASJ. NF-kappaB antiapoptosis: induction of TRAF1 and TRAF2 and c-IAP1 and c- IAP2 to suppress caspase-8 activation. SCI 1998;281:1680–1683.

39. Beg AA, Sha WC, Bronson RT, Ghosh S, Baltimore D. Embryonic lethality and liver degeneration in mice lacking the RelA component of NF-kappa B. Nature 1995;376:167–170. [PubMed: 7603567]

40. Deshmukh M, Johnson EM Jr. Programmed cell death in neurons: focus on the pathway of nerve growth factor deprivation-induced death of sympathetic neurons. Mol Pharmacol 1997;51:897–906. [PubMed: 9187255]

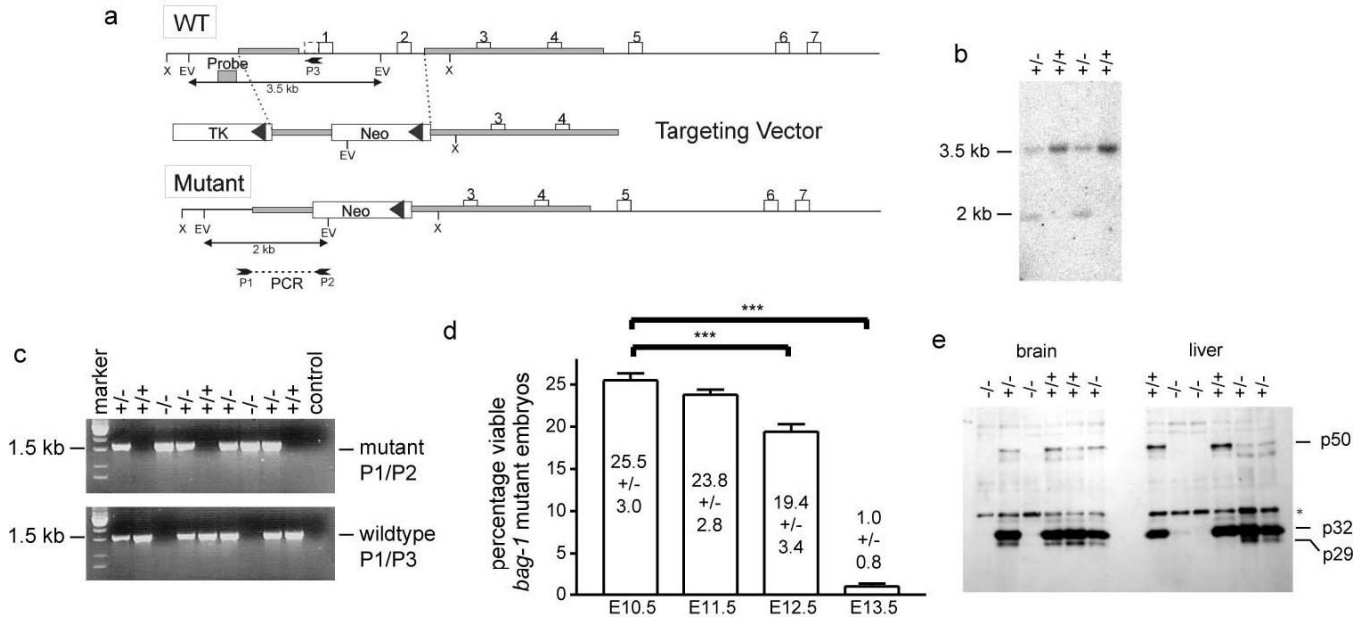

Figure 1. Targeted disruption of *Bag-1* by homologous recombination.

(a) Schematic representation of the *bag-1* genomic locus (WT), the targeting vector, and the mutant allele. The neomycin selectable marker replaces exons 1 and 2 of *bag-1* to generate a null allele. The region recognized by the hybridization probe for Southern analysis and the primer pairs to diagnose the targeted allele are illustrated. X: *Xba*I; EV: *Eco*RV.

(b) Southern blot analysis of ES cell clones. Genomic DNA was digested with *Eco*RV and subjected to Southern blot analysis with the probe indicated in a. The wild-type (WT) allele produced a 3.5 kb fragment, and the targeted allele (KO) a 2 kb fragment. Lanes 1 and 3 show recombinant clones.

(c) PCR analysis of genomic DNA from one litter of a *bag-1*+/− intercross. DNA from 12.5 day old embryos was tested with primer pair P1/P2 to detect the mutant allele and P1/P3 (P3 is deleted in the mutated allele) for the wild-type allele.

(d) Percentage of viable *bag-1*$^{-/-}$ mice at various developmental stages. Whereas the percentage of *bag-1*−/− mice at E10.5 and E11.5 corresponded to the expected 25 %, it was reduced at E12.5 and only 1 % of *bag-1*$^{-/-}$ mice were alive at E13.5.

(e) Western blot analysis (20 μg protein/lane) showed that all Bag-1 protein isoforms (Bag-1L, Bag-1, p29) were absent in brain and liver from *bag-1* wt and mutant E12.5 mouse embryos. The antibody used recognized an additional unspecific band at 35 kd (*).

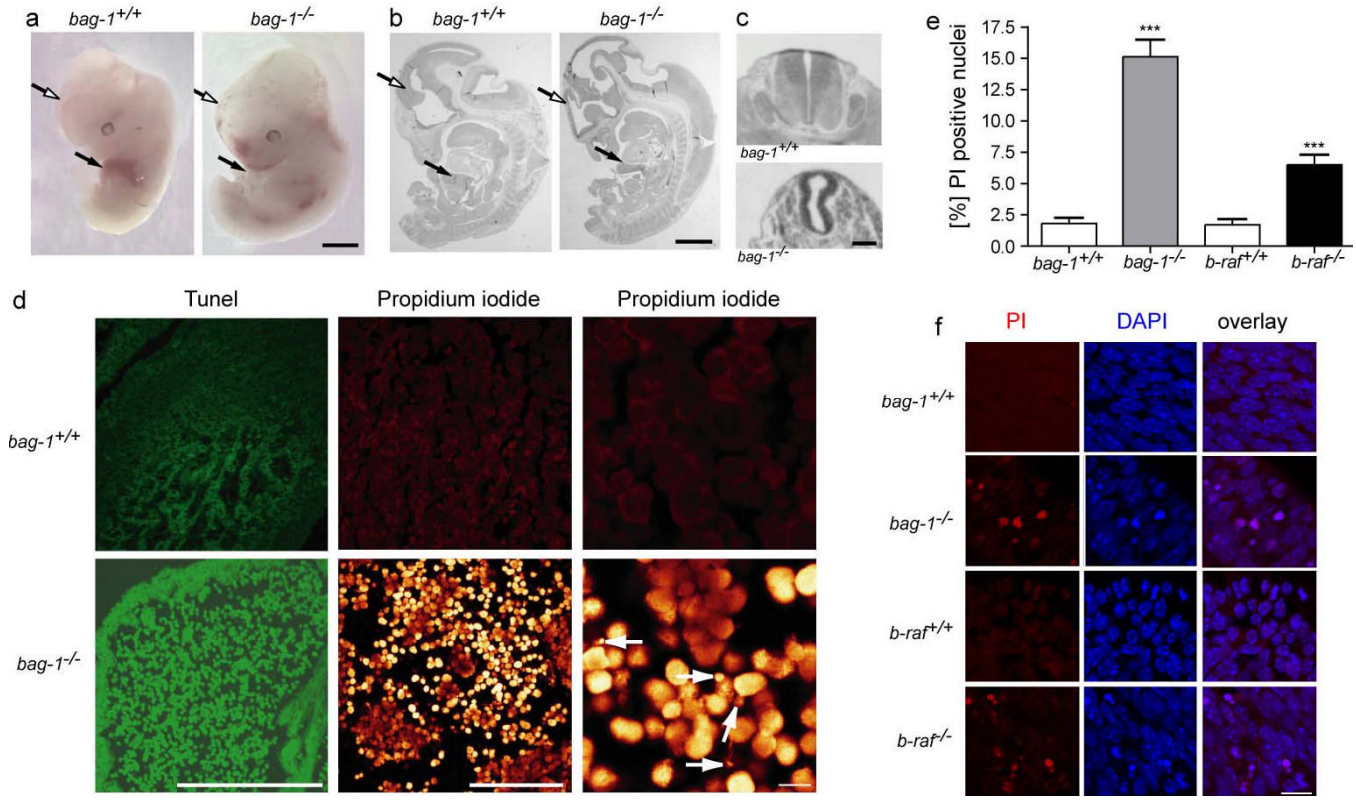

Figure 2. *Bag-1* mutant embryos show severe defects in forebrain and liver.

(a) Embryos from heterozygous *bag-1* intercrosses were dissected at E12.5. The *bag-1*$^{-/-}$ embryos showed massively reduced forebrain thickness (open arrows) and did not show any signs of erythropoiesis in the liver (arrows). Scale bar: 1 mm.

(b) and c) Paraffin sections of *bag-1*$^{+/+}$ and *bag-1*$^{-/-}$ embryos stained with Hemalaun/Eosin. The open arrows point to the forebrain of *bag-1*$^{+/+}$ and *bag-1*$^{-/-}$ embryos and the filled arrows to the liver. c) transverse section through the neural tube of wild-type and *bag-1*$^{-/-}$ embryos at E12.5. Scale bar: 1 mm in b) and 100 μm in c).

(d) Staining for apoptotic cells in the liver with Tunel and Propidium iodide based techniques revealed massive cell death in E12.5 *bag-1*$^{-/-}$ embryos in comparison to *bag-1*$^{+/+}$ littermates. High magnification reveals fragmentating nuclei (arrows) which appear typical of apoptosis. Bars in d): left panel: 100 μm, middle panel: 50 μm, right panel: 10 μm.

(e) Condensed nuclei and Propidium Iodide (PI)-positive cells are increased in E11.5 *bag-1*$^{-/-}$ and *b-raf*$^{-/-}$ embryonic forebrain. Quantification of DAPI/PI-positive cells in the E11.5 embryonic forebrain of *bag-1*$^{+/+}$, *bag-1*$^{-/-}$, *b-raf*$^{+/+}$ and *b-raf*$^{-/-}$ reveals a significant increase in the number of pyknotic /condensed nuclei in *bag-1*$^{-/-}$ and *b-raf*$^{-/-}$ embryos.

(f) Representative high magnification pictures of forebrain areas of the indicated genotypes. Scale bar: 20 μm.

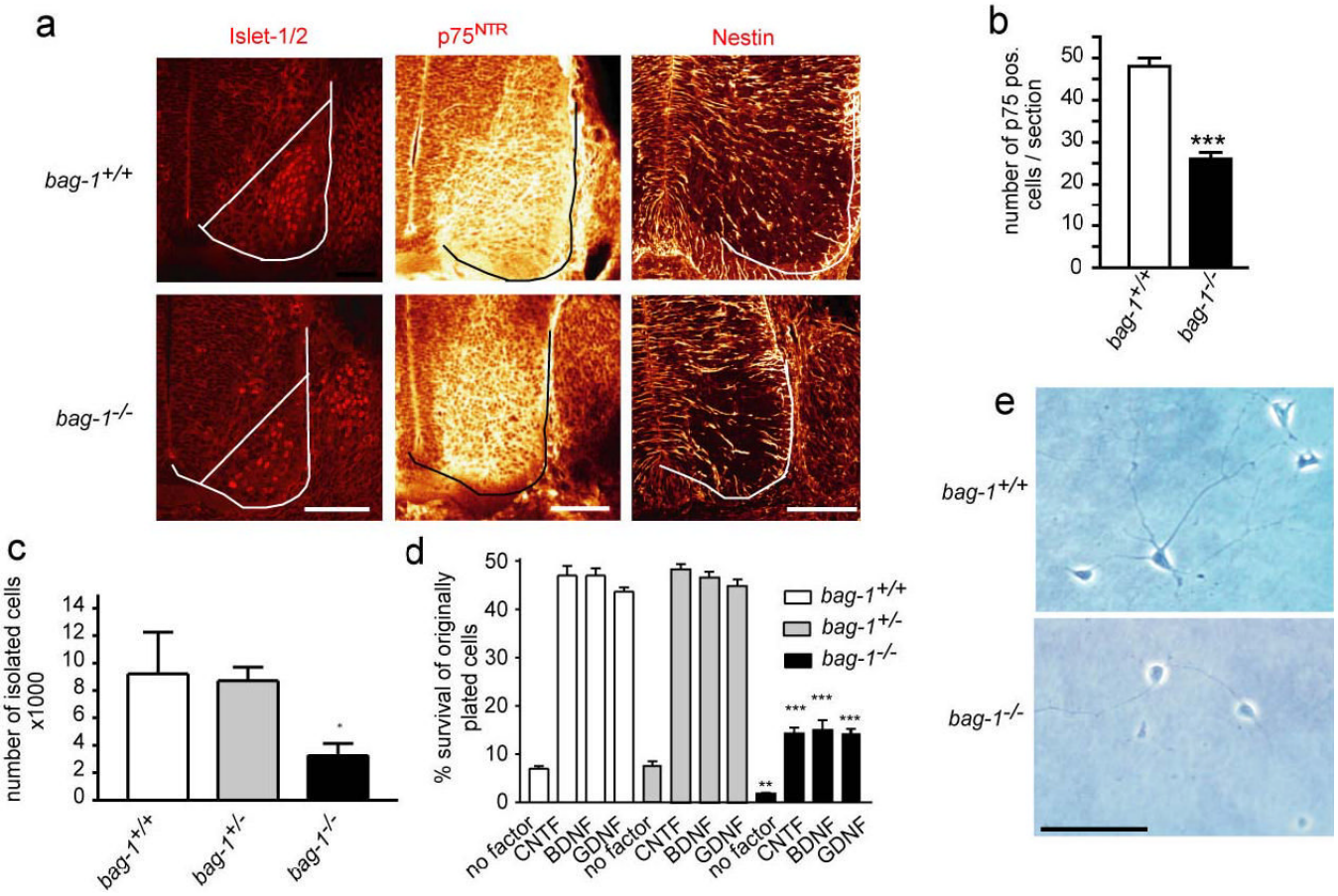

Figure 3. Differentiation and survival of spinal motoneurons is impaired in *bag-1*$^{-/-}$ embryos.

(a) Vibratome sections through the lumbar spinal cord of E11.5 and E12.5 embryos from *bag-1*$^{+/-}$ intercrosses were stained with antibodies against Islet-1/2 (E11.5), p75^{NTR} (E12.5; middle lane) and Nestin (E12.5; right). The line in the left panel marks the border of the neural tube. Staining of motoneuron nuclei for Islet-1/2 and staining for p75^{NTR} neurotrophin receptor or Nestin was reduced in *bag-1*$^{-/-}$ embryos. Bars for all panels: 100 μm.

(b) The number of p75-positive motoneurons counted in serial vibratome sections from *bag-1*$^{-/-}$ mice was significantly reduced.

(c) The number of motoneurons which could be isolated from the lumbar spinal cord of E12.5 *bag-1*$^{-/-}$ embryos was significantly reduced. After a 30 min panning period with p75^{NTR} antibodies, the number of resulting motoneurons was quantified. The number of isolated motoneurons from the spinal cord of *bag-1*$^{-/-}$ was significantly reduced ($P < 0.05$).

(d) Motoneurons were plated at a density of 2000 cells/well and survival was determined after 7 days in culture. Survival rates of *bag-1*$^{-/-}$ motoneurons were significantly reduced (**$P <$ 0.005, ***$P < 0.001$), irrespective of the neurotrophic factor which was added (BDNF, GDNF, CNTF).

(e) Morphology of isolated motoneurons from *bag-1*$^{+/+}$ and *bag-1*$^{-/-}$ embryos after 7 days *in vitro* in the presence of BDNF. The surviving *bag-1*$^{-/-}$ neurons display motoneurons-specific characteristics such as a long axon-like process and shorter dendritic processes. Bar: 100 μm.

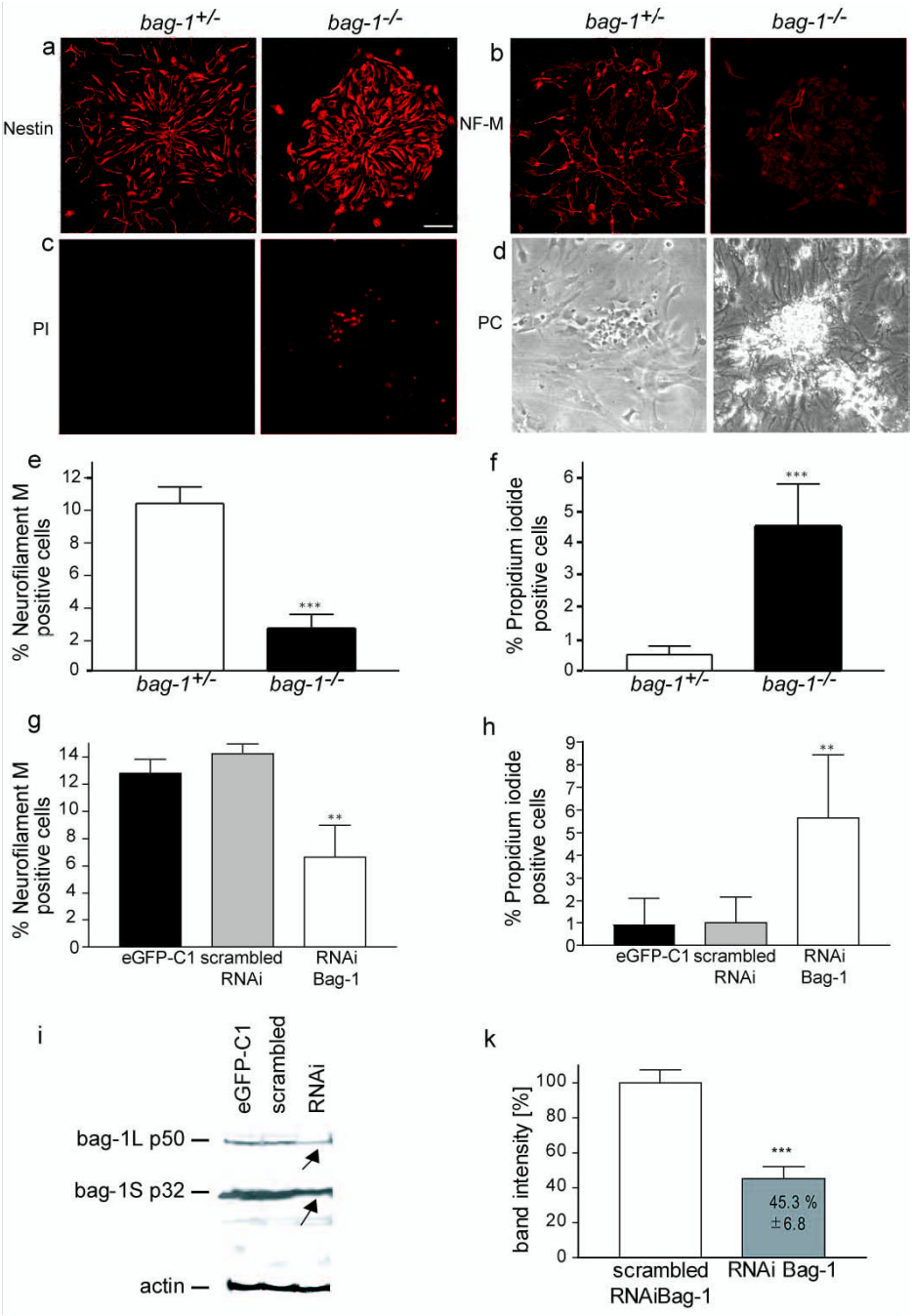

Figure 4. Enhanced apoptosis of differentiating neurons from *bag-1* mutant neural stem cells.

(a) – (d) Neural stem cells were isolated from E11.5 forebrain from *bag-1*$^{+/-}$ intercrosses. Cells from passage 6 were transferred for 24 h to laminin coated dishes, fixed and stained for nestin (a), neurofilament-M (b) and with Propidium iodide (PI; c) Phase contrast pictures for (c) are shown in (d).

(e) Quantitative analysis of neurofilament-positive cells in cultures of differentiating *bag-1*$^{+/+}$ and *bag-1*$^{-/-}$ neural stem cells revealed a significant loss of neurons in *bag-1*$^{-/-}$ cultures. Statistical analysis was carried out by student's t-test: $P < 0.001$.

(f) Quantitative analysis of Propidium iodide-positive cells in cultures of differentiating *bag-1*$^{+/+}$ and *bag-1*$^{-/-}$ neural stem cells. Statistical analysis was performed by students' t-test: $P < 0.001$. Bar: in (b) for (b)–(e): 50 μm.
(g) Quantitative analysis of Propidium iodide-positive cells in differentiating *bag-1*$^{+/+}$ neural stem cell cultures transfected with Bag-1 RNAi, scrambled RNAi or eGFP-C1 vector.
(h) Quantitative analysis of neurofilament-positive cells in cultures of differentiating *bag-1*$^{+/+}$ neural stem cells transfected with Bag-1 RNAi, scrambled RNAi or eGFP-C1 vector.
(i) Western blot analysis for Bag-1 (10 μg protein/lane) from neural stem cells transfected with RNAi (Bag-1), scrambled RNAi or eGFP-C1 vector. Equal loading was controlled by probing the blot with an actin antibody. The Western blot was performed 4 times from independent experiments.
k) Quantification of Bag-1 reduction in neural stem cells after transfection of RNAi Bag-1, in correlation to the expression of Bag-1 in neural stem cells transfected with the scrambled RNAi.

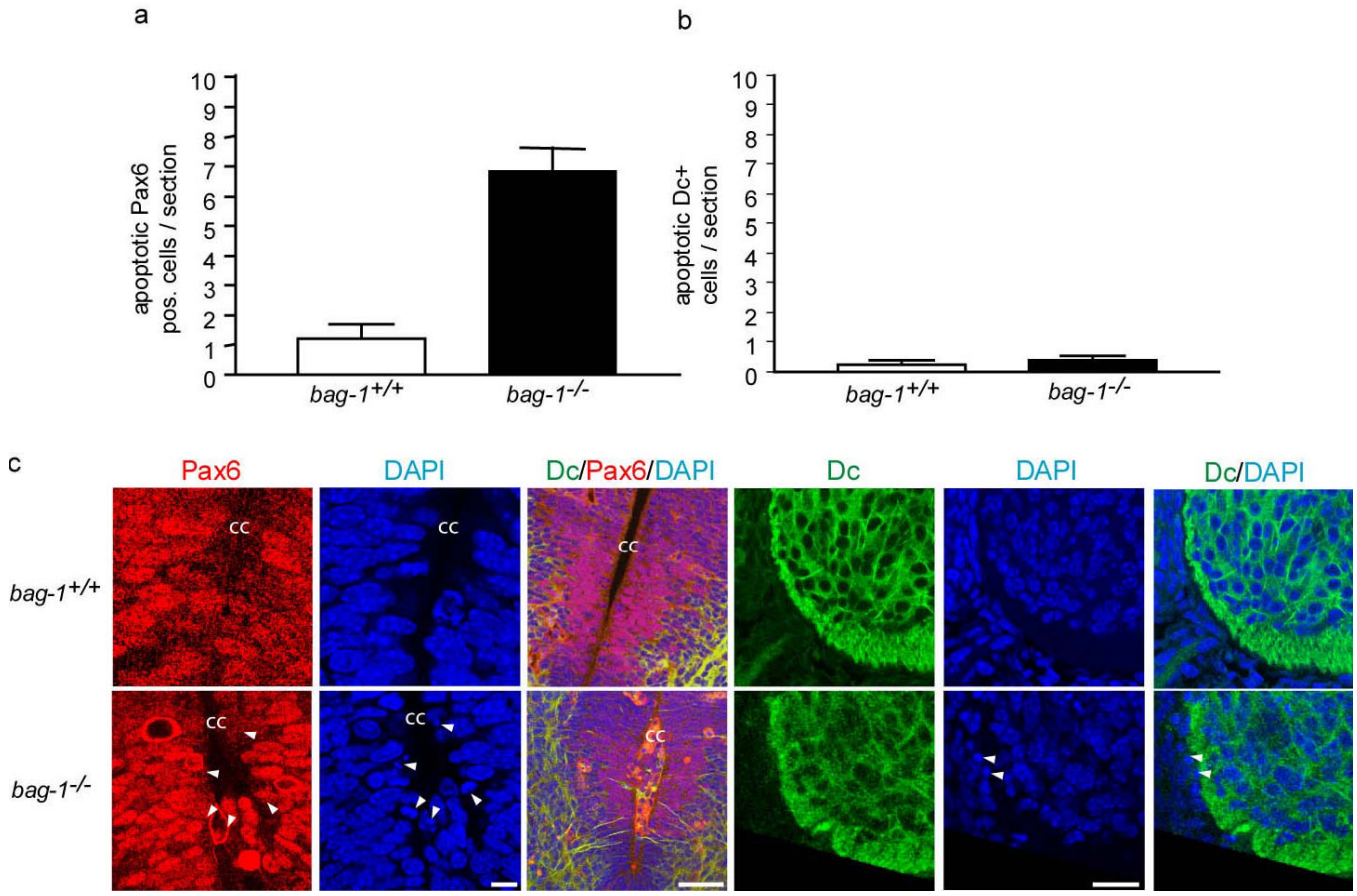

Figure 5. Enhanced apoptosis of differentiating neurons from *bag-1* mutants in the spinal cord.

(a) Quantitative analysis of apoptotic cells in the spinal cord of E11.5 *bag-1*$^{+/+}$ and *bag-1*$^{-/-}$ revealed that increased death in the fraction of Pax6-positive cells.

(b) Apoptosis is not enhanced in the fraction of Doublecortin-positive (Dc) cells in the spinal cord of E11.5 mice. Error bars represent ± SD.

(c) Immunhistochemical detection of Pax6 and Dc in the spinal cord of *bag-1*$^{+/+}$ and *bag-1*$^{-/-}$ embryos (E11.5). DAPI was used as a nuclear marker to identify condensed or fragmented nuclei. Condensed nuclei are marked by arrow heads. Note that condensed nuclei are detectable in the Pax6-positive cell population whereas Dc-positive neural precursor cells only rarely show condensed nuclei. In the third panel from left, triple staining for Pax6, Dc and DAPI is shown at low magnification to demonstrate the distribution of Pax6-positive cells in the neural tube of *bag-1*$^{-/-}$ embryos. A reduction of Pax6-positive cells was particularly evident in more peripheral parts of the neural tube. cc: central canal. Scale bars from left to right: 10 μm, 20 μm and 50 μm.

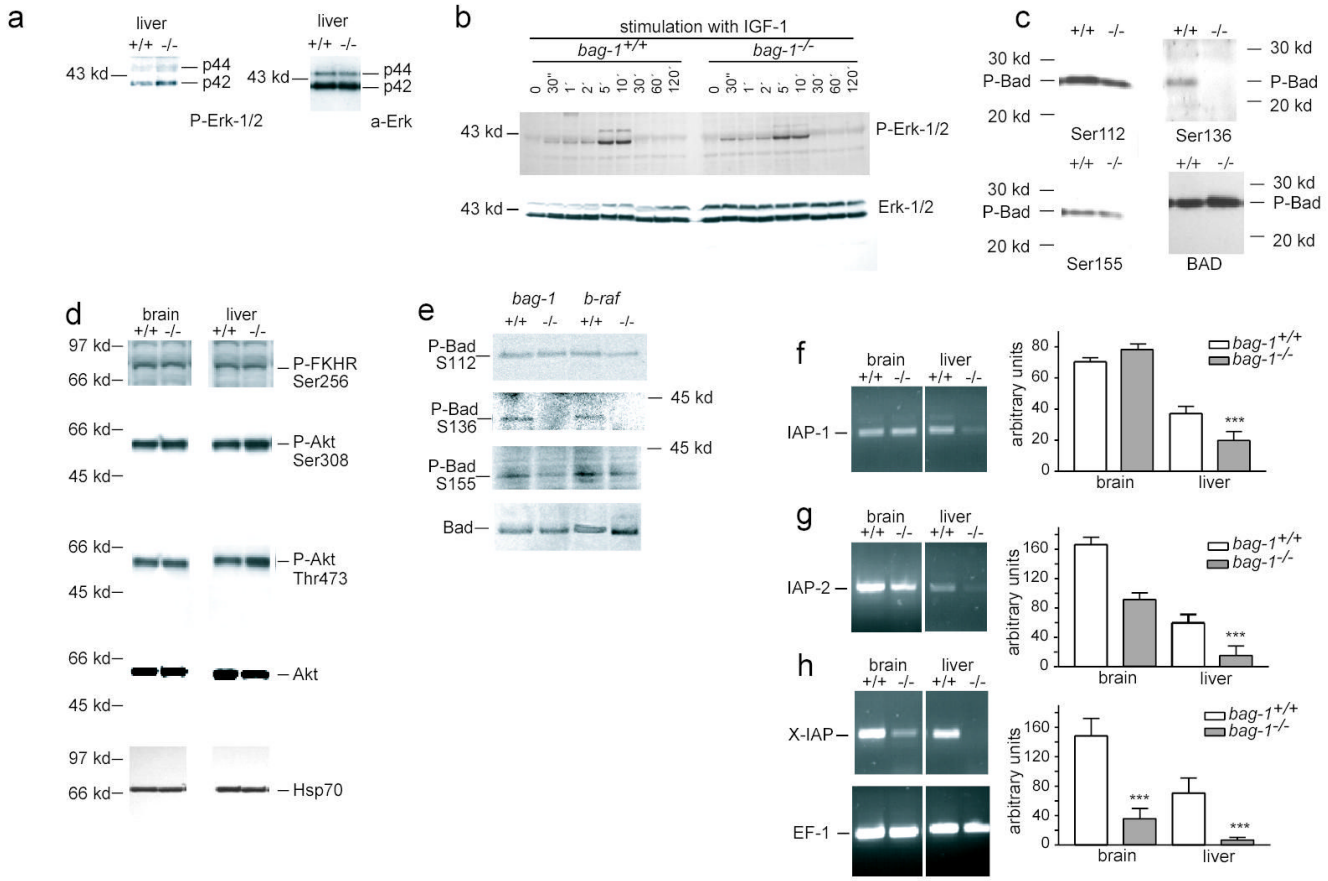

Figure 6. Specific lack of Bad phosphorylation at Ser136 is not caused by inhibiton of MAPK and Akt in *bag-1*$^{-/-}$ embryos.

(a) Phosphorylation of Erk-1/2 is not absent in *bag-1* mutant liver. (a) – (d): Each lane was loaded with 20 μg protein extract.

(b) Protein extracts from serum starved *bag-1*$^{+/+}$ or *bag-1*$^{-/-}$ primary mouse embryonic fibroblasts (PMEF) were stimulated with IGF-1 for time periods (min) as indicated. Western blots probed with Phospho-Erk-1/2 and pan-Erk-1/2 antibodies. Peak phosphorylation of Erk-1/2 was similar at 5 and 10 min for *bag-1*$^{-/-}$ and WT control cells.

(c) Western blots of liver extracts of *bag-1*$^{+/+}$ and *bag-1*$^{-/-}$ mice were probed with anti-Bad-Phospho-Ser112, -136 and -155 and a Pan-Bad antibody, revealing specific absence of phosphorylation at Ser136.

(d) Western blots of single embryo protein extracts were probed with Phospho-Ser256-FKHR, Phospho-Ser473-Akt, Phospho-Thr308-Akt, Akt and Hsp70 antibodies. Each experiment was performed at least 3 times with protein extracts from different mice.

(e) Pull down of Bad from brain extracts of E11.5 *bag-1*$^{+/+}$, *bag-1*$^{-/-}$, *b-raf*$^{+/+}$ and *b-raf* $^{-/-}$ mice probed with the anti-Bad-Phospho-Ser 112, 136, 155 and a Pan-Bad antibody revealing the absence of phosphorylation at Ser136 of Bad.

(f) – (h) IAP expression in brain and liver of *bag-1*$^{-/-}$ embryos. Semi-quantitative analysis of the RT results from E12.5 brain and liver tissue of *bag-1*$^{+/+}$ and *bag-1*$^{-/-}$ is shown on the right, representative RT results are shown on the left. Each set of experiments was performed three times with at least three individual genotypes. Significance was assessed by students' t-test.

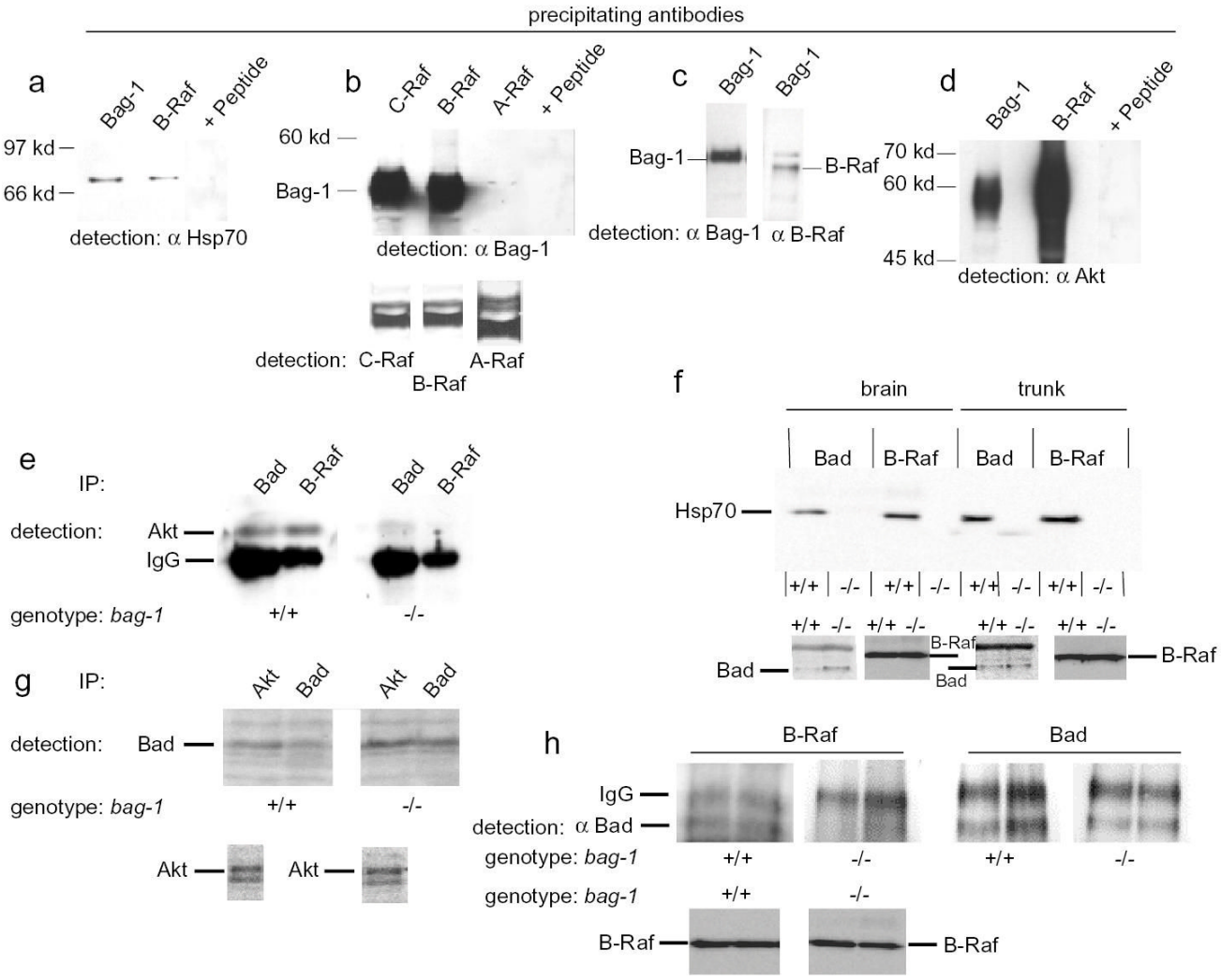

Figure 7. Bag-1 is necessary to form a complex of Bag-1, Hsp70, Raf and Akt.

(a) Immunoprecipitation of endogenous B-Raf and Bag-1 revealed interaction with Hsp70. Addition of the corresponding immunising B-Raf peptide abolished the signal for Hsp70.

(b) C-Raf and B-Raf co-precipitate with Bag-1. A-Raf precipitation did not pulldown Bag-1. Addition of the corresponding peptide for the C-Raf antiserum abolished the signal for Bag-1. Pulldown and detection of the three Raf kinases revealed that they were present.

(c) Bag-1 co-precipitates B-Raf from native PC12 cells. The antiserum against B-Raf cross-reacts with the Ig heavy chain.

(d) Akt co-precipitates with Bag-1 and B-Raf in native PC12 cells. Addition of the corresponding peptide for the B-Raf antiserum abolished the signal for Akt.

(e) Immunoprecipitation of Bad and B-Raf reveals highly reduced interaction between Akt and Bad and lack of interaction between B-Raf and Akt in *bag-1*$^{-/-}$.

(f) Interaction of Hsp70 with Bad and B-Raf is abolished in *bag-1*$^{-/-}$ embryo extracts. Lower panels: loading controls for Bad and B-Raf respectively.

(g) Immunoprecipitation of Akt reveals that Bag-1 is necessary for interaction of this kinase with Bad. In parallel, Bad was precipitated and detected by Western blot to control for Bad protein levels. The lower panel: loading control for Akt.

(h) Immunoprecipitation of B-Raf coprecipitates Bad in *bag-1*$^{+/+}$ but not in *bag-1*$^{-/-}$ embryo extracts (duplicate samples from independent extracts). Bad protein levels are not reduced in extracts from *bag-1*$^{-/-}$ mice. Lower panel: loading control for B-Raf.

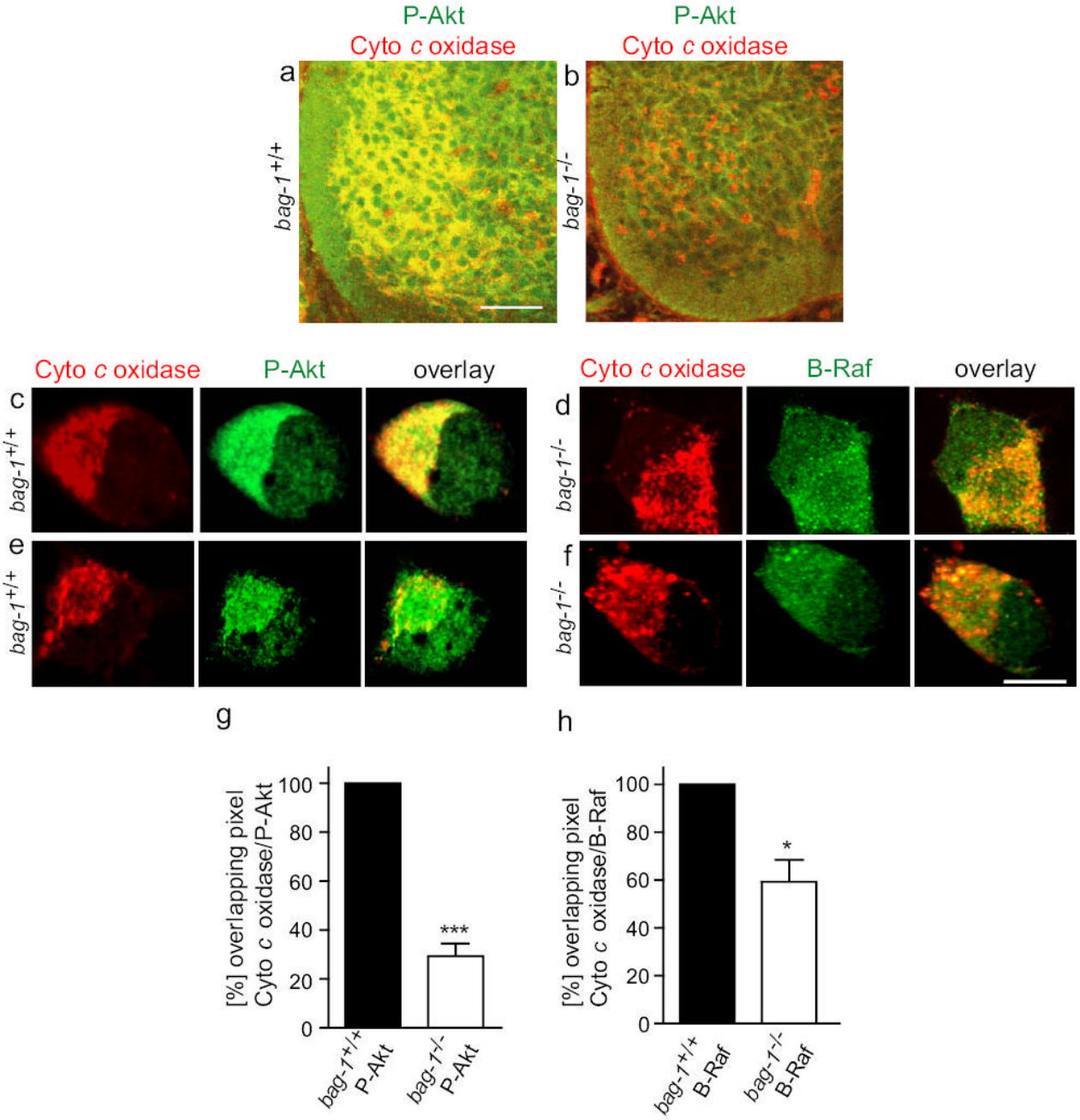

Figure 8. Loss of Bag-1 leads to changes in mitochondrial localization of Akt and Raf in isolated motoneurons.

(a) – (h) Lumbar spinal cord sections and isolated motoneurons from E12.5 *bag-1*$^{+/+}$ (a,c,e) and *bag-1*$^{-/-}$ mice (b,d,f) were fixed with 4 % PFA, stained for Phospho-Akt (red, Cy3, in (a)–(d), B-Raf (red, Cy3, in (e) and (f) and Cytochrome *c* oxidase (green, Cy2, (a)–(f). Akt immunoreactivity appears reduced in the ventrolateral part of the spinal cord in *bag-1*$^{-/-}$ embryos (a), thus reflecting the loss of neurons at E12.5. When motoneurons were isolated and cultured for a short period of 2 days with CNTF and BDNF, the accumulation of P-Akt immunoreactivity at mitochondria was reduced (d) in comparison to WT controls (c). Similarly, B-Raf immunoreactivity which co-localizes with Cytochrome *c* oxidase at mitochondria in

control cells became more dispersed in *bag-1*$^{-/-}$ motoneurons (f). Overlapping pixels of the immunosignal for Cytochrome *c* oxidase (mitochondria) and P-Akt or B-Raf respectively were quantified using a channel plot overlap probability function (Leica TCS2 software). The result shows a reduction in overlay of pixels for P-Akt and Cytochrome *c* oxidase (upper panel) and B-Raf and Cytochrome *c* oxidase (lower panel). Bars: in (a) for (a) and (b): 100 μm; in (f) for (c)–(f): 5 μm.